PHYSICAL REVIEW D **87,** 033005 (2013)

# Mass hierarchy resolution in reactor anti-neutrino experiments: Parameter degeneracies and detector energy response

X. Qian,[1,*] D. A. Dwyer,[1] R. D. McKeown,[2,3] P. Vogel,[1] W. Wang,[3] and C. Zhang[4]

[1]*Kellogg Radiation Laboratory, California Institute of Technology, Pasadena, California 91125, USA*
[2]*Thomas Jefferson National Accelerator Facility, Newport News, Virginia 23606, USA*
[3]*College of William and Mary, Williamsburg, Virginia 23187, USA*
[4]*Brookhaven National Laboratory, Upton, New York 11973, USA*

(Received 7 August 2012; published 15 February 2013)

Determination of the neutrino mass hierarchy using a reactor neutrino experiment at ~60 km is analyzed. Such a measurement is challenging due to the finite detector resolution, the absolute energy scale calibration, and the degeneracies caused by current experimental uncertainty of $|\Delta m^2_{32}|$. The standard $\chi^2$ method is compared with a proposed Fourier transformation method. In addition, we show that for such a measurement to succeed, one must understand the nonlinearity of the detector energy scale at the level of a few tenths of percent.

DOI: 10.1103/PhysRevD.87.033005 PACS numbers: 14.60.Pq

## I. INTRODUCTION AND DEGENERACY CAUSED BY THE UNCERTAINTY IN $\Delta m^2_{\mathrm{atm}}$

Reactor neutrino experiments play an extremely important role in understanding the phenomenon of neutrino oscillation and the measurements of neutrino mixing parameters [1]. The KamLAND experiment [2] was the first to observe the disappearance of reactor anti-neutrinos. That measurement mostly constrains solar neutrino mixing $\Delta m^2_{21}$ and $\theta_{12}$. Recently, the Daya Bay experiment [3] established a nonzero value of $\theta_{13}$. $\sin^2 2\theta_{13}$ is determined to be $0.092 \pm 0.016(\mathrm{stat}) \pm 0.005(\mathrm{sys})$. The large value of $\sin^2 2\theta_{13}$ is now important input to the design of next-generation neutrino oscillation experiments [4,5] aimed toward determining the mass hierarchy (MH) and *CP* phase.

It has been proposed [6,7] that an intermediate L ~ 20–30 km baseline experiment at reactor facilities has the potential to determine the MH. Authors of Refs. [8–10] studied a Fourier transformation (FT) technique to determine the MH with a reactor experiment with a baseline of 50–60 km. Experimental considerations were discussed in detail in Ref. [10]. On the other hand, it has also been pointed out that current experimental uncertainties in $|\Delta m^2_{32}|$ may lead to a reduction of sensitivity in determining the MH [11–13]. Encouraged by the recent discovery of large nonzero $\theta_{13}$, we revisit the feasibility of an intermediate baseline reactor experiment and identify some additional challenges.

The disappearance probability of electron anti-neutrino in a three-flavor model is

$$\begin{aligned} P(\bar{\nu}_e \to \bar{\nu}_e) &= 1 - \sin^2 2\theta_{13}(\cos^2\theta_{12}\sin^2\Delta_{31} + \sin^2\theta_{12}\sin^2\Delta_{32}) \\ &\quad - \cos^4\theta_{13}\sin^2 2\theta_{12}\sin^2\Delta_{21} \\ &= 1 - 2s^2_{13}c^2_{13} - 4c^4_{13}s^2_{12}c^2_{12}\sin^2\Delta_{21} \\ &\quad + 2s^2_{13}c^2_{13}\sqrt{1 - 4s^2_{12}c^2_{12}\sin^2\Delta_{21}}\cos(2\Delta_{32} \pm \phi), \end{aligned} \tag{1}$$

where $\Delta_{ij} \equiv |\Delta_{ij}| = 1.27|\Delta m^2_{ij}|\frac{L(m)}{E(\mathrm{MeV})}$, and

$$\begin{aligned} \sin\phi &= \frac{c^2_{12}\sin 2\Delta_{21}}{\sqrt{1 - 4s^2_{12}c^2_{12}\sin^2\Delta_{21}}} \\ \cos\phi &= \frac{c^2_{12}\cos 2\Delta_{21} + s^2_{12}}{\sqrt{1 - 4s^2_{12}c^2_{12}\sin^2\Delta_{21}}}. \end{aligned} \tag{2}$$

In the second line of Eq. (1), we rewrite the formula using the following notations: $s_{ij} = \sin\theta_{ij}$, $c_{ij} = \cos\theta_{ij}$ and using $\Delta_{31} = \Delta_{32} + \Delta_{21}$ for normal mass hierarchy (NH) and $\Delta_{31} = \Delta_{32} - \Delta_{21}$ for inverted mass hierarchy (IH), respectively. Therefore, the effect of MH vanishes at the maximum of the solar oscillation ($\Delta_{21} = \pi/2$[1]) and will be large at about $\Delta_{21} = \pi/4$. Furthermore, we can define $\Delta m^2_{\phi}(L, E) = \frac{\phi}{1.27}\cdot\frac{E}{L}$ as the effective mass-squared difference, whose value depends on the choice of neutrino energy $E$ and baseline $L$. Since $|\Delta m^2_{32}|$ is only known with some uncertainties ($|\Delta m^2_{32}| = (2.43 \pm 0.13) \times 10^{-3}$ eV$^2$ [14] or more recently $|\Delta m^2| = 2.32^{+0.12}_{-0.08} \times 10^{-3}$ eV$^2$ [15]), there exists a degeneracy between the phase $2\Delta_{32} + \phi$ in Eq. (1) corresponding to the NH and the phase $2\Delta'_{32} - \phi$ corresponding to the IH when a different $|\Delta m^2_{32}|$ (but within the experimental

*Corresponding author.
xqian@caltech.edu

[1]This is true for $\Delta_{21} = n\pi/2$, with $n$ being an integer.

 

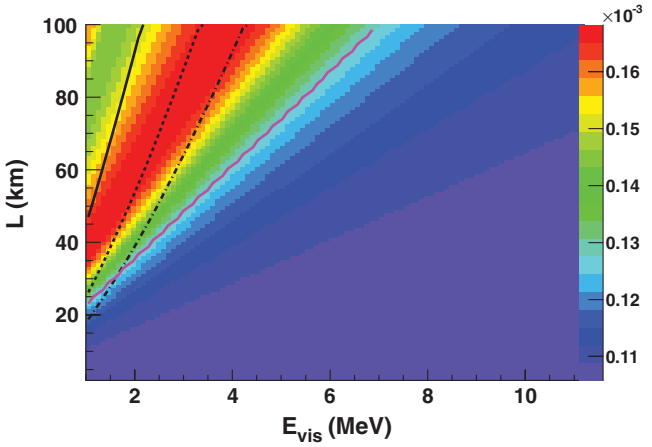


FIG. 1 (color). Map of $\Delta m^2_\phi$ over a phase space of energy and distance. The x axis is the visible energy of the IBD in MeV. The y axis is the distance between the reactor and detector. The legend of color code is shown on the right bar, which represents the size of $\Delta m^2_\phi$ in eV$^2$. The solid, dashed, and dotted lines represent three choices of detector energy resolution with $a =$ 2.6, 4.9, and 6.9, respectively. The purple solid line represents the approximate boundary of degenerate mass-squared difference. See text for more explanations.

uncertainty) is used, namely $\Delta'_{32} = \Delta_{32} + \phi$ at fixed $L/E$.[2] In particular, $\Delta m^2_\phi(60\text{ km}, 4\text{ MeV}) \approx 0.12 \times 10^{-3}$ eV$^2$ (using the experimental values of $\Delta m^2_{21}$ and $\theta_{12}$ [14]), which is similar to the size of the experimental uncertainty of $|\Delta m^2_{32}|$. Thus at fixed $L/E$, determination of mass hierarchy is not possible without improved prior knowledge of $|\Delta m^2_{32}|$.

To some extent, this degeneracy can be overcome by using a range of $L/E$ or actually, as is the case for the reactor neutrinos, a range of neutrino energies $E_{\bar\nu}$. Figure 1 shows the magnitude of $\Delta m^2_\phi$ as a function of distance between reactor and detector ($L$ in km) and the visible energy of the prompt events of inverse beta decay (IBD), which is related to the incident neutrino energy ($E_{\text{vis}} \approx E_{\bar\nu} - 0.8$ in MeV). It is seen that for the region with baseline $L$ below 20 km, the effective mass-squared difference $\Delta m^2_\phi$ remains almost constant for the entire IBD energy range. That indicates an irresolvable degeneracy across the entire spectrum of IBD given the current experimental uncertainty of $|\Delta m^2_{32}|$. At larger distances, $\approx 60$ km, $\Delta m^2_\phi$ exhibits some dependence on energy, indicating that the degeneracy could be possibly overcome, as discussed further below.

With a finite detector resolution, the high-frequency oscillatory behavior of the positron spectrum, whose phase contains the MH information, will be smeared out, particularly at lower energies. For example, at 60 km and 4 MeV, $2\Delta_{32} \approx 30\pi$ for $|\Delta m^2_{32}| = 2.43 \times 10^{-3}$ eV$^2$. Therefore, a small variation of neutrino energy would lead to a large change of $2\Delta_{32}$.

We modeled the energy resolution as

$$\frac{\delta E}{E} = \sqrt{\left(\frac{a}{\sqrt{E(\text{MeV})}}\right)^2 + 1\%}, \tag{3}$$

with choices of $a = 2.6$, 4.9, and 6.9. The values of 4.9% and 6.9% are chosen to mimic achieved energy resolutions of current state-of-the-art neutrino detectors Borexino [16] (5–6%) and KamLAND [17] ($\sim 7\%$), respectively. The value of 2.6% corresponds to an estimated performance for an ideal 100% photon coverage. In reality, a research and development plan to reach the desired detector energy resolution (better than 3% at 1MeV) has been proposed [18]. Our simulation suggests that the lines defined by the relations $2\Delta_{32}\frac{\delta E}{E} = 0.68 \times 2\pi$ represent boundaries of the region where the high-frequency oscillatory behavior of the positron spectrum is completely suppressed. The solid, dashed, and dotted-dashed lines in Fig. 1 show these boundaries for $a = 2.6$, 4.9, and 6.9, respectively. The left side of these lines (lower values of $E_{\text{vis}}$) will yield negligible contributions to the differentiation of MH.

As pointed out above, when $\Delta m^2_\phi$ becomes essentially independent of $E_{\text{vis}}$, the degeneracy related to the $|\Delta m^2_{32}|$ uncertainty makes determination of MH impossible. Again, our simulation suggests that the dividing line is $\Delta m^2_\phi = 0.128 \times 10^{-3}$ eV$^2$, indicated by the purple line in Fig. 1. The right side of this line (larger values of $E_{\text{vis}}$) alone will play very small role in differentiating between these two degenerate solutions. Thus, the region between the steep lines related to the energy resolution and the purple diagonal line related to the degeneracy is essential in extracting the information of the MH. Therefore, at $L < 30$ km it is impossible to resolve the MH while at $L \approx 60$ km there is a range of energies where the affect of MH could be, in principle, visible. At such a distance, the 'solar' suppression of the reactor $\bar\nu_e$ flux is near its maximum and thus the higher frequency and lower amplitude "atmospheric" oscillations become more easily identified.

In order to explore the sensitivity of a potential measurement and simplify our discussion, we assume a 40 GW thermal power of a reactor complex and a 20 kT detector. In the absence of oscillations, the event rate per year at 1 km distance, $R$, is estimated using the results of the Daya Bay experiment [3] to be $R = 2.5 \times 10^8$/year. At a baseline distance of $L$, the total number of events $N$ is then expected to be $N = R \cdot T(\text{year})/L(\text{km})^2 \times \bar P(\bar\nu_e \to \bar\nu_e)$, where $\bar P(\bar\nu_e \to \bar\nu_e)$ is the average neutrino survival probability. Values of mixing angles and mass-squared differences used in the simulation are taken from [3,14]

[2]Other degenerate solutions, naturally, might exist when the uncertainty in $\Delta_{32}$ is larger than $2\pi$.

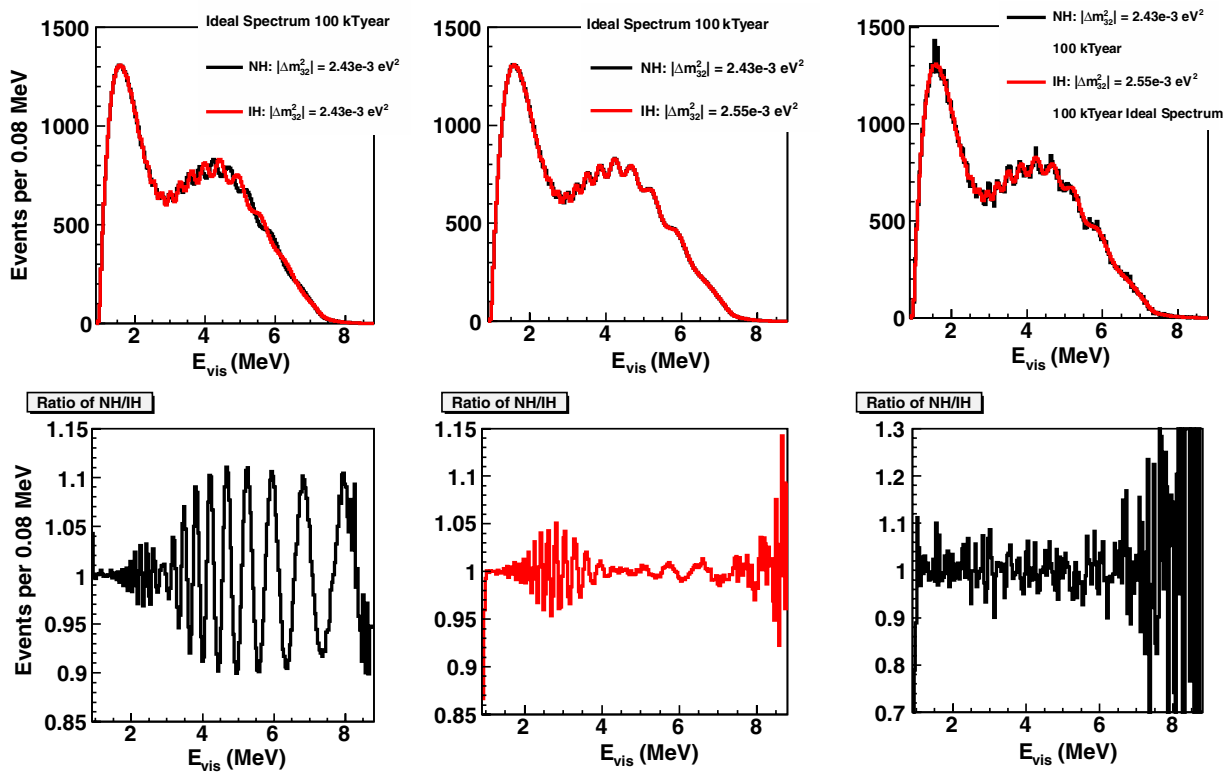


FIG. 2 (color online). Top panels show the comparison of IBD energy spectrum (no statistical fluctuations) with respect to $E_{\rm vis}$ in (MeV) for fixed $|\Delta m^2_{32}| = 2.43 \times 10^{-3}$ eV$^2$ (ideal spectrum in top left), for degenerate $|\Delta m^2_{32}|$ (ideal spectrum in top middle), and degenerate $|\Delta m^2_{32}|$ with 100 kT · year exposure (realistic spectrum in NH case and ideal spectrum in IH case in top right). The ideal spectrum represents the case without any statistical fluctuations, while realistic spectrum includes these statistical fluctuations. The resolution parameter $a$ is chosen to be 2.6. Bottom panels show the ratio of NH to IH case. Due to statistical fluctuations, the range of Y axis in bottom right panel is enlarged to 0.7–1.3 from 0.85–1.15.

$$\begin{aligned} \sin^2 2\theta_{12} &= 0.861^{+0.026}_{-0.022} \\ \Delta m^2_{21} &= (7.59 \pm 0.21) \times 10^{-5}\ \text{eV}^2 \qquad \sin^2 2\theta_{23} \sim 1 \\ |\Delta m^2_{32}| &= (2.43 \pm 0.13) \times 10^{-3}\ \text{eV}^2 \\ \sin^2 2\theta_{13} &= 0.092 \pm 0.017(\text{Daya Bay}). \end{aligned} \tag{4}$$

For example, with five years running at 60 km, the total number of events is about $10^5$. In addition, we assume $a = 2.6$ in Eq. (3). The reactor anti-neutrino spectrum was taken from Ref. [19]. The fuel fractions of $U^{235}$, $U^{238}$, $Pu^{239}$, and $Pu^{241}$ are assumed to be 64%, 8%, 25%, and 3%, respectively.

For the IBD measurement with such a detector, the majority of the backgrounds come from four types of events: the accidental coincidence events, the $Li^9/He^8$ decay events, the fast neutron events, and the geo-neutrino events. The accidental coincidence background can be determined from the experimental data with negligible systematic uncertainties [20–22]. Both the $Li^9/He^8$ decay events and the fast neutron events are caused by cosmic muons. Such backgrounds are significantly suppressed in an experimental site situated deep underground, and their spectra are directly constrained by tagging the cosmic muons [20,21]. The geo-neutrino background with an energy spectrum of $E_{\rm vis} < 2.5$ MeV will give rise to about 3% contamination extrapolated from the measured rate from KamLAND [23] with a 40% relative uncertainty. Since geo-neutrinos originate from U and Th decays, their spectra are very well known and can be included into the spectrum analysis. Overall, we do not expect the backgrounds to pose a significant challenge in resolving the MH. While it will be important to include the effects of backgrounds in a sensitivity calculation for a realistic design, we did not include them in this study.

Figure 2 shows the comparison of the IBD energy spectrum (top panels) and the ratio of NH to IH spectrum (bottom panels) with respect to $E_{\rm vis} \approx E_{\bar{\nu}} - 0.8$ in MeV. It is important to note that we assumed a perfect absolute energy calibration and knowledge of reactor IBD spectrum. Also, the ideal spectrum without statistical fluctuations is considered in the left and middle panels. Compared with the case at known $|\Delta m^2_{32}|$ with no uncertainty (left panels in Fig. 2), the difference between NH and IH can be considerably reduced due to the lack of precise knowledge of $|\Delta m^2_{32}|$ (middle panels in Fig. 2). Furthermore, in right panels of Fig. 2, we show the realistic spectrum of NH with

statistical fluctuations at 100 kT · year exposure together with the ideal spectrum for the IH case. The ratio of these two spectra is shown in the bottom right panel.

In this section we have therefore identified the ambiguities associated with the uncertainty of the $|\Delta m^2_{32}|$ value in relation to the finite detector energy resolution. In particular, we have shown that, under rather ideal conditions (perfect energy calibration, very long exposure, etc.), the corresponding degeneracies can be overcome at intermediate distances ($\sim$ 60 km) and in a limited range of energies.

## II. EXTRACTION OF THE MASS HIERARCHY

In order to study the sensitivity of the mass hierarchy determination under these conditions, we use the $\chi^2$ method together with Monte Carlo simulations to compare the simulated IBD energy spectrum of 100 kT · year exposure with the expected spectrum in both NH and IH cases. The procedure is as follows. First, the simulated spectrum was fit assuming NH by minimizing

$$\chi^2_{\rm NH} = \sum_i \frac{(S^i_m - S^i_{e\,\rm NH}(\Delta m^2))^2}{(\delta S^i_m)^2} + \chi^2_p(\Delta m^2) \qquad (5)$$

with respect to $\Delta m^2$. Here, $S^i_m$ ($S^i_{e\,\rm NH}$) is the measured spectrum (the expected spectrum with NH which depends on value of $\Delta m^2$) at the $i$th bin. The $\delta S^i_m$ is the statistical uncertainty in the $i$th bin. The last term in Eq. (5) is the penalty term from the most recent constrains of $|\Delta m^2_{32}|$ of MINOS ($|\Delta m^2| = 2.32^{+0.12}_{-0.08} \times 10^{-3}$ eV$^2$ [15]). The value of $\Delta m^2$ at the minimum $\chi^2$ is defined as $\Delta m^2_{\rm min\,NH}$. Second, the fit is repeated assuming IH to obtain $\chi^2_{\rm IH}$ and $\Delta m^2_{\rm min\,IH}$. Third, the difference in chi-square values ($\Delta\chi^2$) is defined as

$$\Delta\chi^2 \equiv \chi^2_{\rm NH}(\Delta m^2_{\rm min\,NH}) - \chi^2_{\rm IH}(\Delta m^2_{\rm min\,IH}). \qquad (6)$$

In this procedure, we have neglected the uncertainties of $\Delta m^2_{21}$, $\theta_{12}$, and $\theta_{13}$, as we do not expect them to have a big impact on the MH resolution. First of all, we foresee that the precisions for these parameters will be significantly improved in the future. The uncertainty on $\theta_{13}$ will be determined by the final Daya Bay results to $\sim$5% [22]. The precision of the $\theta_{12}$ and the $\Delta m^2_{21}$ can be improved in this medium-baseline measurement through the neutrino oscillation of solar term [last term in first line of Eq. (1)]. Moreover, the MH determination relies on the frequency measurement rather than the amplitude measurement of the neutrino oscillation. Therefore, it is less sensitive to uncertainties of mixing angles. In addition, since the uncertainty of $\Delta m^2_{21}$ is much smaller than the changes in $\Delta m^2_{\phi}$, it will have negligible impact on the MH resolution as well.

The distributions of $\Delta\chi^2$ for the true NH (black solid line) or IH (dotted red line) are shown in Fig. 3. The area under each histogram is normalized to unity. Furthermore, since the true value of $|\Delta m^2_{32}|$ is not known, the value of

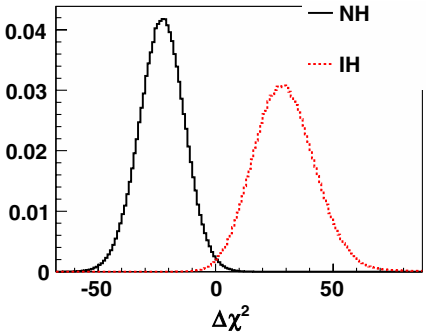


FIG. 3 (color online). The $\Delta\chi^2$ spectrum from Monte Carlo simulation. The NH (IH) represents the case when the nature is normal (inverted) hierarchy.

$|\Delta m^2_{32}|$ used in the simulated spectrum is randomly generated according to the the most recent constrains of $|\Delta m^2_{32}|$ from MINOS. Fourth, given a measurement with a particular value of $\Delta\chi^2$, the probability of the MH being NH case can be calculated as $\frac{P_{\rm NH}}{P_{\rm NH}+P_{\rm IH}}$. The $P_{\rm NH}$ ($P_{\rm IH}$) is the probability density assuming the nature is NH (IH), which can be directly determined from Fig. 3. Finally, the average probability can be calculated by evaluating the weighted average based on the $\Delta\chi^2$ distribution in Fig. 3, assuming the truth is NH. A more detailed description on the average probability can be found in Ref. [24]. With 100 kT · year exposure with resolution parameter $a = 2.6$, the average probability is determined to be 98.9%. Since this average probability is obtained by assuming a perfect knowledge of neutrino spectrum as well as the energy scale, it represents the best estimate for the separation of mass hierarchy.

In order to relax the requirement of knowledge on energy scale and energy spectrum, an attractive Fourier transform (FT) method was proposed recently in Refs. [8–10]. In particular, in Ref. [9] the quantity $(RL + PV)$ is introduced

$$RL = \frac{RV - LV}{RV + LV} \qquad PV = \frac{P - V}{P + V}, \qquad (7)$$

where $P$ is the peak amplitude and $V$ is the amplitude of the valley in the Fourier sine transform (FST) spectrum. There should be two peaks in the FST spectrum, corresponding to $\Delta_{32}$ and $\Delta_{31}$, and the labels $R$, ($L$) refer to the right (left) peak. Simulations in Ref. [10] show that the signs of $RL$ and $PV$ are related to the hierarchy; positive for NH and negative for IH. In addition, in Ref. [10] it was argued that the value of $RL + PV$ is not sensitive to the detailed structure of the reactor IBD spectrum nor to the absolute energy calibration.

In Fig. 4, we plot the central values of $(PV + RL)$ for a range of $|\Delta m^2_{32}|$ and for both hierarchies with the pre-2011 flux [19,25–28] and the new reevaluated flux [28–30]. Although the general feature of $(PV + RL)$ (positive for NH and negative for IH) is confirmed, the $|\Delta m^2_{32}|$ dependence of $(PV + RL)$ value is shown to depend on the

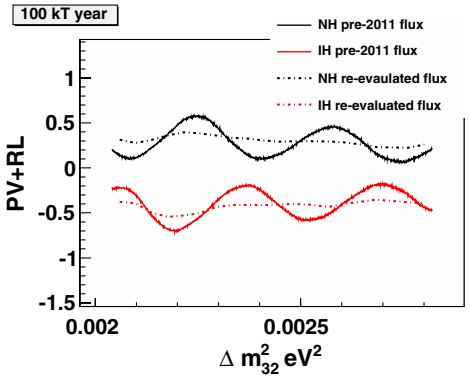


FIG. 4 (color online). Values of $(RL + PV)$ for a range of $|\Delta m^2_{32}|$ and both hierarchies are plotted for the 100 kT · year exposure with both pre-2011 flux and the reevaluated flux.

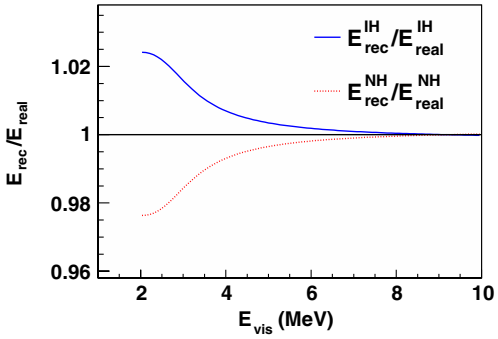


FIG. 5 (color online). The ratio of $E_{\rm rec}$ to $E_{\rm real}$ for the case of IH based on Eq. (8) (solid line) is shown with respect to the visible energy $E_{\rm vis}$. The dotted line shows the ratio of $E_{\rm rec}$ to $E_{\rm real}$ for the case of NH.

choices of flux model. In addition, as we emphasized in Fig. 1 when trying to determine the MH, one should not use just one fixed value of $|\Delta m^2_{32}|$ for comparison of the NH case with the IH case (as was done in Refs. [9,10]) but consider all possible values of $|\Delta m^2_{32}|$ within the current experimental uncertainties. The observed oscillation behavior with pre-2011 flux would lead to a reduction in the probability to determine the MH. With the Monte Carlo simulation procedure using $(PV + RL)$, the average probability is determined to be 93% with the pre-2011 flux. Furthermore, the average probability is expected to be smaller than that from the full $\chi^2$ method in general, since the FT method utilizes less information (e.g., only heights of peaks and valleys) in order to reduce the requirement in energy scale determination. Figure 4 shows that a good knowledge of the neutrino flux spectrum is desired to correctly evaluate the probability of MH determination with the FT method.

## III. CHALLENGES OF THE ENERGY SCALE

As stressed in the discussion of Fig. 1, in the energy interval $E_{\rm vis} = 2$–$4$ MeV (at $L = 60$ km), the quantity $\Delta m^2_\phi$ changes significantly with respect to the uncertainty in $|\Delta m_{32}|^2$. The lower limit of that region is caused by the smearing of the fast oscillations of the observed spectrum due to the finite detector energy resolution, while the upper limit is caused by the degeneracy, i.e., by the fact that $\Delta m^2_\phi$ becomes almost independent of energy from that value on. All of these are then reflected in the FT analysis. Although the FT method does not require an absolute calibration of energy scale [10], a precision calibration of the relative energy scale is extremely important. A small nonlinearity of the energy scale characterization can lead to a substantial reduction of the discovery potential.

To illustrate this point, we consider the case corresponding to IH and assume that (due to imperfect understanding of the detector performance) the reconstructed energy $E_{\rm rec}$ is related to the real energy $E_{\rm real}$ by the relation

$$E_{\rm rec} = \frac{2|\Delta' m^2_{32}| + \Delta m^2_\phi(E_{\bar\nu}, L)}{2|\Delta m^2_{32}| - \Delta m^2_\phi(E_{\bar\nu}, L)} E_{\rm real}. \tag{8}$$

(Here we use the notation $|\Delta' m^2_{32}|$ and $|\Delta m^2_{32}|$ to emphasize the fact that $|\Delta m^2_{32}|$ is known only within a certain error.) If the energy scale is distorted according to this relation, and that distortion is not included in the way the reconstructed energy is derived from the data, the pattern of the disappearance probability regarding the atmospheric term will be exactly the same as in the NH case. This can be seen as

$$\cos\left((2|\Delta m^2_{32}| - \Delta m^2_\phi(E_{\bar\nu}, L))\frac{L}{E_{\rm real}}\right) = \cos\left((2|\Delta' m^2_{32}| + \Delta m^2_\phi(E_{\bar\nu}, L))\frac{L}{E_{\rm rec}}\right) \tag{9}$$

from Eq. (1). In this case the analysis of the spectrum would lead to an obviously wrong MH. Since the exact value of $|\Delta m^2_{32}|$ is not known, we must consider in Eq. (8) all allowed values of $|\Delta' m^2_{32}|$ including those that minimize the ratio $E_{\rm rec}/E_{\rm real}$.

Figure 5 shows the ratio $E_{\rm rec}/E_{\rm real}$ versus the visible energy (solid line) with the energy scale distortion described by Eq. (8) where $|\Delta' m^2_{32}|$ was chosen so that this ratio is one at high $E_{\rm vis}$. Comparing the medium energy region ($2$ MeV $< E_{\rm vis} < 4$ MeV) with the higher energy region ($E_{\rm vis} > 4$ MeV), the average $E_{\rm rec}/E_{\rm real}$ is larger than unity by only about 1%. In addition, the same argument similar to Eq. (8) applies to the NH case as well. The ratio $E_{\rm rec}/E_{\rm real}$ versus the visible energy (dotted line) of NH is also shown in Fig. 5. Therefore, to ensure the MH's discovery potential from such an experiment, the nonlinearity of energy scale $(E_{\rm rec}/E_{\rm real})$ needs to be controlled to a fraction of 1% in a wide range of $E_{\rm vis}$. This requirement should be compared with the current state-of-the-art 1.9% energy scale uncertainty from KamLAND [31]. Therefore, nearly an order of magnitude improvement in the energy scale determination is required for such a measurement to succeed.

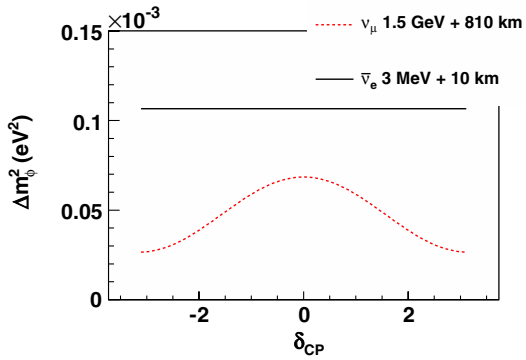


FIG. 6 (color online). The dependence of effective mass-squared difference $\Delta m^2_{ee\phi}$ (solid line) and $\Delta m^2_{\mu\mu\phi}$ (dotted line) with respect to the value of $\delta_{CP}$ for $\bar{\nu}_e$ and $\nu_\mu$ disappearance measurements, respectively.

## IV. UNCERTAINTIES IN $|\Delta m^2_{32}|$

The current primary method to constrain $|\Delta m^2_{32}|$ is the $\nu_\mu$ disappearance experiment. However, similar to the $\bar{\nu}_e$ disappearance case as in Eq. (1), the $\nu_\mu$ disappearance measurement in vacuum[3] would also measure an effective mass-squared difference rather than $|\Delta m^2_{32}|$ directly. The corresponding effective mass-squared difference is smaller than that in the $\bar{\nu}_e$ case, basically since in Eq. (2) the cosine squared of $\theta_{12}$ is replaced by the sine squared. Also, in this case, the effective mass-squared difference will depend not only on $\Delta_{21}$, $\theta_{12}$, but also on $\theta_{13}$, $\theta_{23}$, as well as on the unknown $CP$ violation phase $\delta_{CP}$. The effective mass-squared differences from $\nu_\mu$ and $\nu_e$ disappearance with respect to the value of $\delta_{CP}$ are shown in Fig. 6. The difference in $\Delta m^2_\phi$ between the $\nu_\mu$ and $\nu_e$ channels actually opens a new path to determine the MH. This possibility was discussed earlier in Refs. [32,33]. It was stressed there that the difference in frequency shifts $2\Delta_{32} \pm \phi$ has opposite signs for the $\bar{\nu}_e$ and $\nu_\mu$ disappearance in the normal or inverted hierarchies. Such a measurement would require that $2\Delta_{32} \pm \phi$ is measured to a fraction of $\Delta m^2_{ee\phi} - \Delta m^2_{\mu\mu\phi}$ level ($5 \times 10^{-5}$ eV$^2$) in both channels. In the current $\sim$60 km configuration, the knowledge of $|\Delta m^2_{32}|$ enters through the penalty term in Eq. (5). Therefore, in order for knowledge of $|\Delta m^2_{32}|$ to have a significant impact on the determination of MH, the $\Delta_{32} \pm \phi$ in $\nu_\mu$ channel should also be measured to a fraction of $\Delta m^2_{ee\phi} - \Delta m^2_{\mu\mu\phi}$ level, which is well beyond the reach of T2K [34] and NO$\nu$A [35] $\nu_\mu$ disappearance measurements.[4]

## V. CONCLUSIONS

In summary, the sensitivity of determining the neutrino mass hierarchy using the reactor neutrino experiment at $\sim$60 km is explored and its challenges are discussed. Such a measurement is difficult due to the finite detector energy resolution, to the necessity of the accurate absolute energy scale calibration, and to degeneracies related to the current experimental uncertainty of $|\Delta m^2_{32}|$. The key to the success of such a measurement is to control the systematic uncertainties. We show here that one must understand the nonlinearity of the detector energy scale to a few tenths of percent, which requires nearly an order of magnitude of improvement in the energy scale compared to the current state-of-the-art limit, 1.9% from KamLAND.

## ACKNOWLEDGMENTS

We would like to thank Liang Zhan and Jiajie Ling for fruitful discussions. This work was supported in part by Caltech, the National Science Foundation, and the Department of Energy under Contracts No. DE-AC05-06OR23177, under which Jefferson Science Associates, LLC, operates the Thomas Jefferson National Accelerator Facility, and No. DE-AC02-98CH10886.

[3]In practice, the uncertainty in the matter effect would introduce only a systematic uncertainty. The strength of the effect in $\nu_\mu$ disappearance is close to that of changing $|\Delta m^2_{32}|$ by a few times of $10^{-6}$ eV$^2$.

[4]The projected 1-$\sigma$ uncertainties on $|\Delta m^2| = |\Delta m^2_{32} \pm \Delta m^2_{\mu\mu\phi}/2|$ from T2K and NO$\nu$A are about $5.3 \times 10^{-5}$ eV$^2$.

[1] R. D. McKeown and P. Vogel, Phys. Rep. **394**, 315 (2004).
[2] K. Eguchi *et al.*, Phys. Rev. Lett. **90**, 021802 (2003).
[3] F. P. An *et al.*, Phys. Rev. Lett. **108**, 171803 (2012).
[4] T. Akiri *et al.*, arXiv:1110.6249.
[5] D. Angus *et al.*, arXiv:1001.0077.
[6] S. T. Petcov and M. Piai, Phys. Lett. B **533**, 94 (2002).
[7] S. Choubey, S. T. Petcov, and M. Piai, Phys. Rev. D **68**, 113006 (2003).
[8] J. G. Learned, S. T. Dye, S. Pakvasa, and R. C. Svoboda, Phys. Rev. D **78**, 071302(R) (2008).
[9] L. Zhan, Y. Wang, J. Cao, and L. Wen, Phys. Rev. D **78**, 111103(R) (2008).
[10] L. Zhan, Y. Wang, J. Cao, and L. Wen, Phys. Rev. D **79**, 073007 (2009).
[11] A. Gouvêa, J. Jenkins, and B. Kayser, Phys. Rev. D **71**, 113009 (2005).

[12] H. Minakata, H. Nunokawa, S. J. Parke, and R. Z. Funchal, Phys. Rev. D **76**, 053004 (2007).
[13] S. J. Parke, H. Minakata, H. Nunokawa, and R. Z. Funchal, Nucl. Phys. B, Proc. Suppl. **188**, 115 (2009).
[14] K. Nakamura (Particle Data Group), J. Phys. G **37**, 075021 (2010).
[15] P. Adamson *et al.*, Phys. Rev. Lett. **106**, 181801 (2011).
[16] G. Alimonti *et al.*, Nucl. Instrum. Methods Phys. Res., Sect. A **600**, 568 (2009).
[17] C. Zhang, Ph.D. thesis, Caltech, 2011.
[18] Y. F. Wang, NuFact12, Williamsburg, VA, USA (2012), https://www.jlab.org/indico/materialDisplay.py?contribId=160&sessionId=4&materialId=slides&confId=0.
[19] P. Vogel, G. K. Schenter, F. M. Mann, and R. E. Schenter, Phys. Rev. C **24**, 1543 (1981).
[20] F. P. An *et al.*, Nucl. Instrum. Methods Phys. Res., Sect. A **685**, 78 (2012).
[21] F. P. An *et al.*, Chinese Phys. C **37**, 011001 (2013).
[22] X. Qian (Daya Bay Collaboration), arXiv:1211.0570.
[23] T. Araki *et al.*, Nature (London) **436**, 499 (2005).
[24] X. Qian, A. Tan, W. Wang, J. J. Ling, R. D. McKeown, and C. Zhang, Phys. Rev. D **86**, 113011 (2012).
[25] F. Von Feilitzsch, A. A. Hahn, and K. Schreckenbach, Phys. Lett. **118B**, 162 (1982).
[26] K. Schreckenbach, G. Colvin, W. Gelletly, and F. V. Feilitzsch, Phys. Lett. **160B**, 325 (1985).
[27] A. A. Hahn, K. Schreckenbach, W. Gelletly, F. V. Feilitzsch, G. Colvin, and B. Krusche, Phys. Lett. B **218**, 365 (1989).
[28] V. Kopeikin, L. Mikaelyan, and V. Sinev, Phys. At. Nucl. **67**, 1892 (2004).
[29] Th. A. Mueller *et al.*, Phys. Rev. C **83**, 054615 (2011).
[30] P. Huber, Phys. Rev. C **84**, 024617 (2011).
[31] S. Abe *et al.*, Phys. Rev. Lett. **100**, 221803 (2008).
[32] H. Minakata, H. Nunokawa, S. J. Parke, and R. Z. Funchal, Phys. Rev. D **74**, 053008 (2006).
[33] H. Nunokawa, S. J. Parke, and R. Z. Funchal, Phys. Rev. D **72**, 013009 (2005).
[34] Y. Itow *et al.*, arXiv:hep-ex/0106019.
[35] NO$\nu$A Collaboration, http://www-nova.fnal.gov.